A NONITERATIVE METHOD FOR CALCULATING BEAM POSITON FROM INDUCED ELECTRIC SIGNALS*

Eva S. Bozoki, Jung-Yun Huang,+ John W. Bittner
Brookhaven National Laboratory
Upton New York 11973

Abstract

The PUE's in the NSLS storage rings are of the 4 button type. Near the center of the PUE the beam position can be well approximated with a linear function of the sum and the difference signals induced on these electrodes by the bunched beam. The nonlinear response of the PUE's further away from the center was measured. An algorithm was developed to compensate for this effect.

1. Introduction

With more and more sophisticated experiments and the installation of insertion devices, the need for stability of the electron beam orbit in the NSLS storage rings has increased over the past few years. This requires more accurate measurement and better control of the orbit. As part of the effort to be able to control the beam orbit to ≈50μ accuracy, new method of orbit correction was worked out [1] and the orbit monitor electronics is being upgraded [2].

It has become increasingly important to develop an algorithm that can be used to correct for the nonlinearities in the beam position measuring system. With the aid of a bench measurement we have developed such an algorithm. The present paper describes this effort.

2. Determination of Beam Displacement

2.1 The closed orbits in the NSLS storage rings are measured using sets of four circular pickup electodes (PUE's) mounted on the rectangular vacuum chamber as shown of Fig. 1.

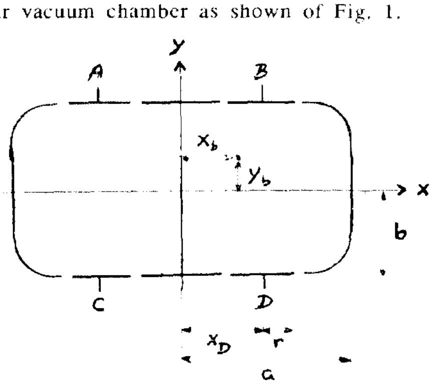

Fig. 1 The NSLS vacuum chamber with pickup electrodes (PUE's).

The electron bunches passing by the PUE's induce V_a, V_b, V_c, V_d voltages on the electrodes, which are sampled sequentially by switches. The signals are detected by a fixed frequency receiver tuned to a harmonic of the RF frequency.**

The x_b horizontal and y_b vertical orbit displacements of the beam are then calculated from the sums and differences of the signals as:

$$x_b = K_x x_e \tag{1a}$$

$$y_b = K_y y_e \tag{1b}$$

K_x and K_y in the above equations have the dimension of lengths, and in general they depend on the x_b, y_b beam position, thus making the (1a,b) relationships nonlinear. In practice, K_x, K_y can be considered constants only near the center of the vacuum chamber.

The x_e, y_e "electrical coordinates" in eqs.(1) are defined as

$$x_e = \frac{(V_b + V_d) - (V_a + V_c)}{V_a + V_b + V_c + V_d} = \frac{V_x}{V_s}$$

$$y_e = \frac{(V_a + V_b)}{V_a + V_b + V_c + V_d} = \frac{V_y}{V_s}$$

Further information may be obtained by the remaining combination of the four induced signals:

$$\Delta = \frac{(V_b + V_c)}{V_a + V_b + V_c + V_d} = \frac{V_\Delta}{V_s}$$

2.2 One could calculate the x_e, y_e "electrical coordinates" as a function of the x_b, y_b beam position (see Appendix) by solving the corresponding Dirichlet problem either analytically [4,5] or using the POISSON (or any similar) program. The resulting equations, do not lend themselves easily to inversion. However it is possible to solve for the x_b, y_b beam positions with an iterative method [5].

A slightly different approach is to use bench measurements to approximate the $K_{x,y}(x_b, y_b)$ functions and then solve the implicit eqs.(1) with a recursive method [6].

2.3 Another, more direct way of solving the problem is to use the bench measurements to approximate K_x and K_y as a function of the measured "electrical coordinates", thus transforming eqs.(1) from implicit to explicit relations, thereby avoiding iterative process.

Besides being able to avoid recursive methods, an additional benefit of using calibration measurements is that all actual deviation from the ideal case (effects of the finite transverse size of the beam, sensor geometry errors, gain error in the electronics or any distortion introduced by the electronics [5]) are taken into account.

3. Bench Measurement

3.1 An aluminium antenna of ≈ 3 mm diameter, simulating the beam, was inserted longitudinally into a section of the vacuum chamber with the four PUE electrodes in place. A movable slide mount allowed positioning the antenna in the x and y transversal directions with an accuracy of ≈ 10 μ. For PUE signal detection the newly developed electronics [2] was used, the outputs of which were the V_x, V_y and V_Δ voltages while the V_s sum voltage was kept constant. The accuracy of the V_x, V_y, V_Δ was ≈.005 Volts (corresponding to ≈15 μ movement in the antenna position). The antenna was connected to an RF source at 211.54 MHz (the same frequency to which the PUE signal receiver was tuned).

The vacuum chamber was scanned along x_b = constant lines and measurements were made with the antenna positioned at x_b = 0, ±1, ±2, ±5, ±10, ±15, ±20, ±25, ±29 mm and y_b = 0, ±1, ±2, ±5, ±8, ±11 mm grid-points. The antenna used in the measurements had a short shield, ≈16 mm in diameter, attached to its base which precluded measurements beyond these positions.

3.2 After correcting for small offset between the mechanical and electrical zero-points, we found that x_e and y_e are symmetrical around $x_b = 0$ and $y_b = 0$.

Therefore, it is justified to simplify calculations in the followings and look at only a quadrant of the vacuum chamber using the averaged x_e and y_e values.

3.3 Fig. 2a shows y_e as a function of x_e. The horizontal lines correspond to measurements at y_b = constant, while the vertical lines correspond to x_b = constant. One can see how the original orthogonal x_b, y_b grid is distorted.

---

*Work performed under the auspices of the U.S. Department of Energy
+Permanent address: Pohang Light Source, Pohang Institute of Science and Technology, Korea.
**At the present time there are two kinds of actual implementation; some of the PUE's are using the old electronic circuits [3], some the new one.

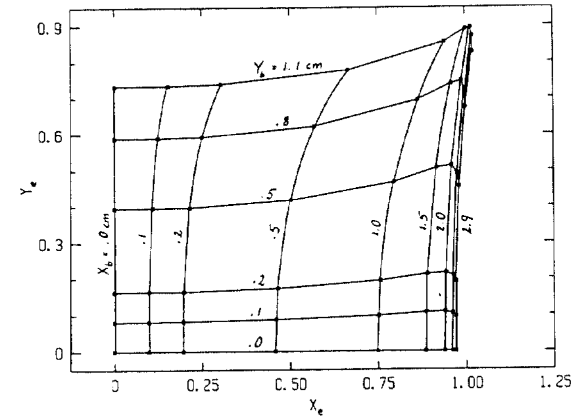

Fig. 2a y_e as function of x_e showing strongly nonlinear behaviour. Horizontal and vertical lines correspond to y_b = constant and x_b = constant, respectively.

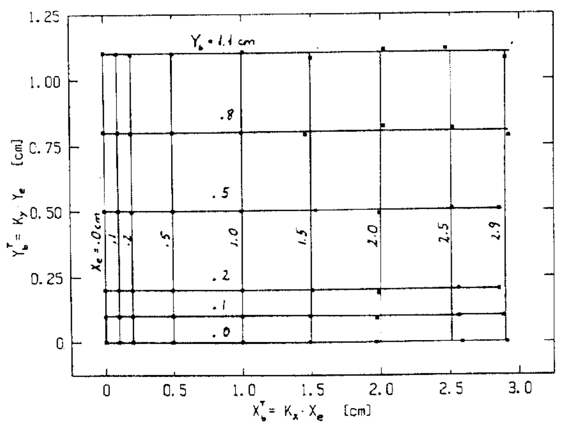

Fig. 2b Reconstructed x_b^T, y_b^T grid, where K_x and K_y were calculated using the (3) Taylor series expansion up to 7-th order terms.

1. Even at $y_b = 0$, x_b does not seems to be linearly dependent on x_e for $x_b \geq 5$ mm. The Δx_e distances between the equidistant Δx_b lines are dramatically decreasing with increasing x_b,

2. The nonlinearity starts at smaller x_b's as y_b is increased.

3. For y_e, the nonlinearity is less pronounced even up to $y_b \approx 11$ mm for small x_b's (≤ 5 mm). This can also be seen from Table 1 (see explanation later).

Using the results of an analytic solution of the Dirichlet problem as guidance, the measured x_e, y_e and Δ points were fitted in the form given by eqs.(6) in the Appendix. Using only the first seven terms in the sums, the agreement is good; the RMS difference between measured and fitted values are $\leq .002$, $\leq .020$ and $\leq .015$ for x_e, y_e and Δ, respectively.

Figs. 3, 4 and 5 show the 3D plots of the $x_e(x_b, y_b)$, $y_e(x_b, y_b)$ and $\Delta(x_b, y_b)$ functions as fitted. The corresponding 2D projections are also shown on the figures. This presentation clearly visualizes the properties described in connection with Fig.2a.

3.4 Let us now turn to the inverse problem which arises when one has to calculate the unknown beam position from the measured electrical coordinates. As one can see from Figs. 3, at large displacements ($x_b \geq 20$ mm) a small error in x_e can result in a large uncertainty in x_b, and unfortunately one can not resolve the uncertainty any better using information provided by Δ.

As we have already stressed, it is not a trivial task to invert the (6a,b) relations given in the Appendix. Therefore we are looking for the fitting function in a Taylor expanded form. Simple symmetry considerations, similar to relations (2) and the conditions that x_b and y_b should be zero along the y_e and x_e axis, respectively (i.e. $x_b(x_e = 0, y_e) = 0$ and $y_b(x_e, y_e = 0) = 0$) suggest that the Taylor expansion should be of the form:

$$x_b^T = \sum_{m=0}^{M}\sum_{n=0}^{m} a_{m,n} x_e^{2m+1-2n} y_e^{2n} \qquad y_b^T = \sum_{m=0}^{M}\sum_{n=0}^{m} b_{m,n} x_e^{2n} y_e^{2m+1-2n}$$

and

$$= x_e \sum_{m=0}^{M}\sum_{n=0}^{m} a_{m,n} x_e^{2m-2n} y_e^{2n} \qquad = y_e \sum_{m=0}^{M}\sum_{n=0}^{m} b_{m,n} x_e^{2n} y_e^{2m-2n}$$

$$= x_e K_x(x_e, y_e) \qquad = y_e K_y(x_e, y_e) \tag{2}$$

(The x_b^T, y_b^T notation is used to distinguish between the actual and the calculated beam positions). The $a_{m,n}$ and $b_{m,n}$ coefficients were obtained from fitting the bench measured data with the (3) Taylor series.

To show the goodness of the approximation, the beam position was calculated for each measured gridpoint from eqs.(1) using

(i) constant K_x, K_y and

(ii) their Taylor approximation (up to 7-th order terms), using the fitted values of the a and b coefficients.

The constant K_x and K_y were calculated to yield $x_b^T = y_b^T = 1$ mm when the antenna position was $x_b = y_b = 1$ mm. The RMS differences between measured and calculated beam positions for both cases are given in Table-1. The results are shown separately for two regions within the vacuum chamber; inside and outside an ± 5 by ± 5 mm rectangle around the middle of the vacuum chamber. Even in the center region, the error in the beam position calculation, assuming linear behaviour (constant K's), is in the order or larger than the required $\approx 50\ \mu$ accuracy.

Table-1
RMS differences between measured and calculated beam position using constant $K_{x,y}$ or their Taylor approximation for the center and for the outside region of the vacuum chamber (up to 7-th order terms).

	center region		outside region	
	Taylor	Constant	Taylor	Constant
Δx_{RMS} [mm]	$7.8\ 10^{-3}$	$7.9\ 10^{-2}$	$1.8\ 10^{-1}$	8.96
Δy_{RMS} [mm]	$5.2\ 10^{-3}$	$4.8\ 10^{-2}$	$2.4\ 10^{-2}$	$7.1\ 10^{-1}$

The results in Table-1 show that it was possible to fit the bench measured data in the form of the (3) Taylor series to very good accuracy. The calculated y_b^T were plotted as a function of x_b^T on Fig. 2b, where as on Fig. 2a, the horizontal and vertical lines correspond to y_b = constant and x_b = constant, respectively. One can see, that the original orthogonal x_b, y_b grid is well reconstructed.

In future orbit measurements the fitted values of the $a_{m,n}$ and $b_{m,n}$ coefficients will be used to calculate the x_b, y_b beam positions from the measured x_e, y_e's.

Appendix

Following the treatment presented in [4], the charge induced by a passing electron bunch with the electrodes short circuited to the wall is calculated first. Then the real response is obtained by regarding the electrodes as current generators in parallel with the capacities of the electrodes to the wall and to each other.

Assuming that the walls of the vacuum chamber are on uniform potential, and in case of a relativistic and infinitely thin beam, the scalar Φ potential satisfying the Dirichlet problem for the rectangle (see Fig.1) is [4,7]:

$$\Phi(x, y) = \frac{\rho}{a}\sum \frac{sh[\alpha_m(b+y)]sh[\alpha_m(b \pm y_b)]}{\alpha_m sh(2b\alpha_m)} \times \sin[\alpha_m(a+x_b)]\sin[\alpha_m(a+x)] \tag{3}$$

where ρ is the beam density localized at (x_b, y_b) and $\alpha_m = m\pi / 2a$. In eq. (4) $\pm y_b$ is used if $y > y_b$ or $y \leq y_b$, respectively. The electric field, normal to the walls at $y = \pm b$ is

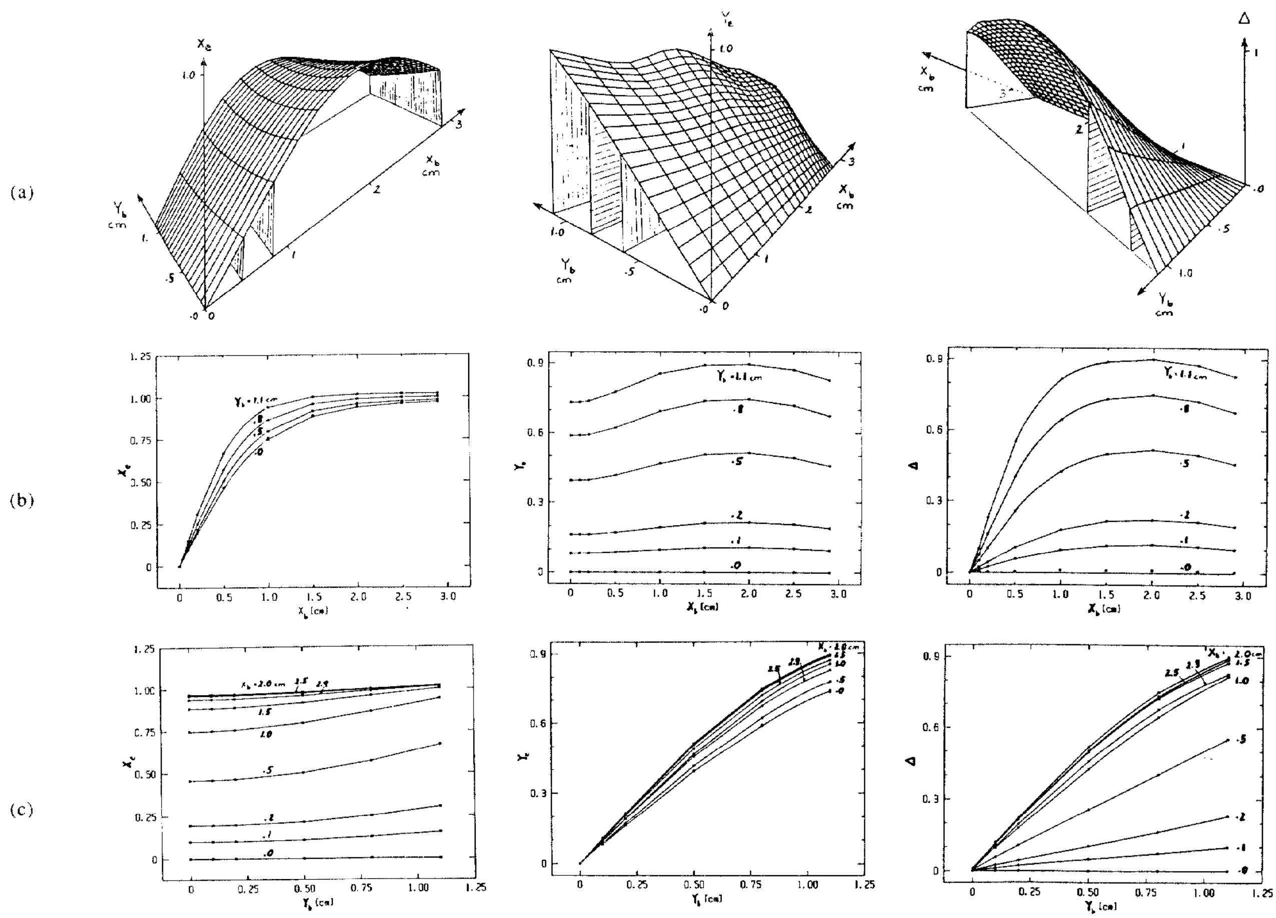

Figs. 3 Figs. 4 Figs. 5

The F = x_e , y_e and Δ functions are shown vs. the (x_b , y_b) beam position as 3D-plots (Figs. a), as well as their two 2D-projections onto the F, x_b and F, y_b planes (Figs. b and c). The functions were obtained by fitting the bench measured points in the form of eqs. (6), representing the solution of the Dirichlet problem for a rectangle.

$$(E_n) = -\left(\frac{\partial\Phi}{\partial y}\right)_{y=\pm b}$$

$$= -\frac{\rho}{a}\sum \frac{\mathrm{sh}\left[\alpha_m(b \pm y_b)\right]}{\mathrm{sh}(2b\alpha_m)} \sin\left[\alpha_m(a + x_b)\right] \sin\left[\alpha_m(a + x)\right] \quad (4)$$

yielding an induced voltage on an electrode located at x and having a radius of r:

$$V = \frac{q}{C} = -\frac{i}{cC}\int_{x-r}^{x+r} (E_n)_{y=\pm b}\, dx$$

where Q is the total charge induced on the electrode, i is the instantenous bunch current, c is the speed of light and C is the capacity of the electrode to the other electrodes and to the wall.

One can take advantage of the fact that the electrodes are at symmetrical positions to simplify the calculations. Since:

$$x_A = x_C = -x_B = -x_D = |x| \quad \text{and} \quad y_A = y_B = -y_C = -y_D = b$$

certain terms cancel each other in the sums and differences and one obtains:

$$x_e = \frac{V_x}{V_s} = \frac{\sum A_{2m} \sin(\alpha_{2m}x_b)\mathrm{ch}(\alpha_{2m}y_b)}{\sum B_{2m+1} \cos(\alpha_{2m+1}x_b)\mathrm{ch}(\alpha_{2m+1}y_b)} \quad (5a)$$

$$y_e = \frac{V_y}{V_s} = \frac{\sum C_{2m+1} \cos(\alpha_{2m+1}x_b)\mathrm{sh}(\alpha_{2m+1}y_b)}{\sum B_{2m+1} \cos(\alpha_{2m+1}x_b)\mathrm{ch}(\alpha_{2m+1}y_b)} \quad (5b)$$

$$\Delta = \frac{V_\Delta}{V_s} = \frac{\sum D_{2m} \sin(\alpha_{2m}x_b)\mathrm{sh}(\alpha_{2m}y_b)}{\sum B_{2m+1} \cos(\alpha_{2m+1}x_b)\mathrm{ch}(\alpha_{2m+1}y_b)} \quad (5c)$$

where the A_m , B_m , C_m , D_m coefficients depend only on the geometry.

Acknowledgements

The authors wish to express their gratitude to John Galayda for many stimulating discussions, to Klaus Halbach whose valuable advice helped us greatly and to Richard Biscardi for his cooperation on problems of electronics.

References

[1] L.H. Yu, E.S. Bozoki, J. Galayda, S. Krisnsky, and G. Vignola, Real time harmonic closed orbit correction schemes, presented at the 1989 Particle Accelerator Conf. in Chicago.

[2] R. Biscardi and J.W. Bittner, Switched detector for beam position monitor, presented at the 1989 Particle Accelerator Conf. in Chicago.

[3] E.S. Bozoki, J.W. Bittner, L. Blumberg, T. Dickerson, J. Galayda, Closed Orbit Correction of the NSLS VUV Ring, Proceedings, 1983 Particle Accelerator Conference, IEEE Trans. on Nucl. Sci. Vol. 30, No. 4, 1983.

[4] J.H. Cuperus, Monitoring of particle beams at high frequencies, NIM 145, 1977, p. 219.

[5] Klaus Halbach, Description of beam position monitor signals with harmonic functions and their Taylor series expansions, NIM A260, 1987, p. 14.
[6] A. Aragona et al., Measurement and steering of beam position in ADONE, INFN-LNF-87/16(P), 1987.
[7] John D. Jackson, Classical Electrodynamics, Wiley & Sons Inc., 1975, p. 121.